Cell. Mol. Life Sci. 65 (2008) 2431 – 2444
1420-682X/08/152431-14
DOI 10.1007/s00018-008-8135-x

Cellular and Molecular Life Sciences

Research Article

Molecular diversity and evolution of cystine knot toxins of the tarantula *Chilobrachys jingzhao*

J. Chen[†], M. Deng[†], Q. He[†], E. Meng, L. Jiang, Z. Liao[+], M. Rong and S. Liang[*]

The Key Laboratory of Protein Chemistry and Developmental Biology of Ministry of Education, College of Life Sciences, Hunan Normal University, Changsha 410081 (P.R. China), Fax: +86-731-8861304, e-mail: liangsp@hunnu.edu.cn

Received 15 March 2008; received after revision 7 May 2008; accepted 4 June 2008
Online First 26 June 2008

Abstract. Cystine knot toxins (CKTs) in spider venoms represent a rich source of novel ligands for varied ion channels. Here, we identified 95 novel putative CKT precursors by analyzing expressed sequence tags of the tarantula *Chilobrachys jingzhao* venom gland. Phylogenetics analyses revealed one orphan family and six families with sequence similarity to known toxins. To further investigate the relationships of their structures, functions and evolution, we assayed 10 representative toxins for their effect on ion channels, and performed structure model comparisons, evolution analysis and toxin distribution analysis. This study revealed two major types of CKTs: pore-blocking toxins and gating modifier toxins. A few blockers were observed with relatively high abundance and wide distribution, which may be a category of original toxins that block channels conserved in various preys with relatively high specificity. The gating modifier families contain advanced toxins, usually have many members and interact with diverse regulatory components of channels.

Keywords. Toxin, molecular diversity, classification, pore-blocking, gating modifier, evolution.

Introduction

Over 30 000 spider species have been found in the world and most of them are equipped with venomous glands. Tarantulas, comprising more than 860 species, like all other spiders are predators that feed on a variety of vertebrate and invertebrate prey [1]. Tarantulas do not use webs for capture, but are well-equipped predators, possessing a variety of venoms that target receptors in the nervous system, probably with adaptation to a certain type of prey [2, 3]. This ability to paralyze higher vertebrates makes these venoms interesting substances for the study of vertebrate receptors [3, 4]. Cystine knot toxins (CKTs) are among the most extensively studied constituents of spider venoms. They are small, compact molecules cross-linked by three to five disulfide bonds, and have molecular masses ranging from 3.5 to 7 kDa. The properties and structures of toxins from spider venoms have been reviewed in detail [3, 5–7]. Tarantulas use two major scaffolds as templates to develop their "pharmaceutical factory", namely the inhibitor cystine knot (ICK) [8, 9], which is also referred to as knottin [10], and less prominently, the disulfide-directed β-hairpin (DDH)-derived fold [11, 12].
However, the classification and evolution of tarantula CKTs remain uncertain [13], possibly due to lack of

[†] These authors contributed equally to this work.
[+] Present address: Marine Science College of Zhejiang Ocean University, Zhoushan 316004 (P.R. China)
[*] Corresponding author.

sequence data, especially full-length cDNA information. The sequence alignments and clusters based on short mature peptides, which usually are saturated in amino acid replacement, cannot provide clear clues for classification and evolution. These problems frustrate research on both the molecular diversity and the genetic mechanisms of toxin evolution, which are of great importance towards understanding this pharmacological arsenal and planning its future use [4].

The tarantula *Chilobrachys jingzhao* is one of the most venomous spiders living in southern China. In our recent work, 60 peptides were purified by ion-exchange and reversed-phase high-performance liquid chromatography and sequenced fully or partially by Edman degradation sequencing [14]. However, most of their full-length precursors, and thus their peptide sequences, are still unknown and their functions have not been systematically elucidated. In this article, we report the results of sequencing a cDNA library from the venom gland of the spider that includes 74 groups (95 sequences) of CKTs. Using patch-clamp techniques, the functions of 10 representative toxins of various families were systematically assayed. We further explored the molecular diversity, classification and characteristics of the toxins in regard to modification, structure, and evolution. All the cDNA sequences are available for public view in the Animal Toxin Database (ATDB) (http://protchem.hunnu.edu.cn/toxin) [15] and in the GenBank database of NCBI (http://www.ncbi.nlm.nih.gov/entrez, accession numbers: EU233831–EU233934).

Materials and methods

cDNA library construction and expression sequence tags sequencing

The tarantula *C. jingzhao* was collected in Hainan province of China. The preparation of total RNA was performed as the previously described [16]. The venomous glands of eight female spiders of the same age and from the same region were harvested and homogenized in liquid nitrogen, followed by cell lysis in the presence of TRIzol reagent (Invitrogen). Polyadenylic acid (+) [polyA(+)] RNA was purified from the total RNA on an oligo(dT)-cellulose affinity column using the mRNA Purification Kit (Promega) according to the manufacturer's protocol. The full-length cDNA library was constructed as described by the instructions provided with the Creator™ SMARTTM cDNA Library Construction Kit (Clontech).

The polymerase chain reaction was performed with the M13 forward and reverse primers in the kit to rapidly screen recombinant clones. The clones containing inserts $\geq$500 base pairs were grown in LB medium containing chloramphenicol (30 μg/mL) in 96-well plates for 16 h. The plasmids were extracted by alkaline lysis and sequenced from the 5′-end on an automated ABI PRISM 3700 sequencer (Perkin Elmer) using the T7 promoter primer and ABI PRISM® Big Dye™ terminator v3.1 ready reaction cycle sequencing kits (Applied Biosystems).

Sequence and structure analysis

cDNA sequencing outputs were trimmed by removal of vector, primer sequences and poly(A) tails with ABI PRISM®DNASequencing Analysis SoftwareV.3.3 [17]. The consensus sequences of each cluster were further filtered by screening for homology to ribosomal RNA, mitochondrial DNA and *E. coli* genome sequences [18, 19]. After deleting matches, the remaining sequences were searched against public databases (nr/NCBI, SwissProt/UniProtKB and TrEMBL/UniProtKB) using the BLASTn or BLASTx programs to identify putative functions of the new expression sequence tags (ESTs) [20]. The signal peptides were predicted with the SignalP 3.0 program (http://www.cbs.dtu.dk/services/SignalP/). Furthermore, the putative CKTs were searched in KNOTTIN database (http://knottin.cbs.cnrs.fr) [10, 21]. Multiple sequences of precursors were aligned using the ClustalW program [22, 23]. The resulting alignments were then hand-edited using the BioEdit program (http://www.mbio.ncsu.edu/BioEdit/BioEdit.html).

Seven known structure models of toxins (1I25 of HWTX-II, 1Y29 of HWTX-X, 1LUP of GsMTX-2, 2I1T of JZTX-III, 1ZJQ of JZTX-VII, 2A2V of JZTX-XI and 1EIT of mu-Agatoxin) were downloaded from PDB database [24]. The predicted structures were modeled using MODELLER software [25] based on known structures (JZTX-VIII from HWTX-II; JZTX-50 from HWTX-X; JZTX-V from GsMTX-2; JZTX-55 from mu-Agatoxin). Pymol software [26] was used to visualize these structures.

Electrophysiological assays

Toxins were purified and identified as described previously [14]. Acutely dissociated dorsal root ganglion (DRG) cells were prepared from 4-week-old Sprague-Dawley rats and maintained in short-term primary culture using the method described by Xiao et al. [27, 28]. Briefly, the dissociated cells were suspended in essential Dulbecco's modified Eagle's medium (DMEM) containing trypsin (0.5 g/L, type III), collagenase (1.0 g/L, type IA), and DNase (0.1 g/L, type III) and incubated at 34 °C for 30 min. Trypsin

inhibitor (1.5 g/L, type II-S) was used to terminate enzyme treatment. The DRG cells were transferred to 35-mm culture dishes (Corning, Sigma) containing 95 % DMEM, 5 % newborn calf serum, hypoxanthine aminopterin thymidine supplement, and penicillin-streptomycin and then incubated in the CO_2 incubator (5 % CO_2, 95 % air, 37 °C) for 1–4 h before the patch-clamp experiment.

Ionic currents were recorded from DRG cells under whole-cell patch-clamp condition using an EPC-9 patch-clamp amplifier (HEKA Electronics, Germany) at room temperature (20–25 °C). The patch pipettes with resistances of 2–3 MΩ were fabricated from borosilicate glass tubing (VWR micropipettes, 100 µl, VWR Company) using a two-stage vertical microelectrode puller (PC-10, Narishige, Japan) and fire-polished by a heater (Narishige, Japan). Voltage steps and data acquisition were controlled using a PC computer with software Pulsefit + Pulse 8.0 (HEKA Electronics, Germany). The P/4 protocol was used to subtract linear capacitive and leakage currents. The series resistance compensation was applied to 70–80 % to minimize voltage errors.

Calcium currents were measured using Ba^{2+} as a charge carrier. The external solution contained: 160 mM triethanolamine-Cl, 10 mM HEPES, 2 mM $BaCl_2$, 10 mM glucose, and 200 nM tetrodotoxin, adjusted to pH 7.4 with triethanolamine-OH. The internal solution contained: 120 mM $CsCl_2$, 5 mM Mg-ATP, 0.4 mM Na_2-GTP, 10 mM EGTA, and 20 mM HEPES-CsOH (pH 7.2) [29]. Ba^{2+} current was evoked at –50 or 0 mV from a holding potential of –90 or –40 mV.

For sodium current recordings, the bath solution contained: 150 mM NaCl, 2 mM KCl, 5 mM D-glucose, 1 mM $MgCl_2$, 1.5 mM $CaCl_2$, and 10 mM HEPES at pH 7.4; the pipette internal solution contained: 105 mM CsF, 35 mM NaCl, 10 mM HEPES, and 10 mM EGTA at pH 7.4. Sodium currents were elicited at –10 mV from a holding potential of –80 mV.

For potassium current recordings, the bath solution contained: 160 mM NaCl, 4.5 mM KCl, 2 mM $CaCl_2$, 1 mM $MgCl_2$ and 10 mM HEPES, pH 7.4 (with NaOH); The internal pipette solution contained: 155 mM KF, 2 mM $MgCl_2$, 10 mM EGTA and 10 mM HEPES, pH 7.2 (with KOH). Currents were elicited by a depolarizing voltage of +10 mV when cells were held at –80 mV.

Evolutionary analysis

Sequences were aligned using ClustalW (Version 1.82) [22], and gapped positions were omitted from subsequent analyses. The nucleotide sequences of different domains including signal peptides, propeptides, and mature peptides of family D and E were aligned. The number of synonymous substitutions per synonymous site (Ds) and the number of nonsynonymous substitutions per nonsynonymous site (Dn) were estimated using the original Nei-Gojobori model (p-distance) [30]. The Fisher's exact tests for positive evolution (based on the original Nei-Gojobori model) were carried out using MEGA software [31].

Results

Considerable numbers of CKTs and classification

From the cDNA library of *C. jingzhao* venom gland, 886 ESTs sequenced and 95 predicted novel CKT precursors were obtained. A full-length CKTs precursor usually contains a signal peptide, a propeptide and a mature peptide; moreover, some precursors also contain an additional tail region. However, to the best of our knowledge, it is still difficult to determine the endoproteolytic sites anterior to mature peptides of seven precursors (JZTX-67, 68, 69, 70, 71, 72 and 74). Most of precursors can be spliced and modified during the post-translational processes, which has also been found in some other toxins and appears to be important for transportation, biological activity and degradation protection [32]. Therefore, comprehensive analysis of full-length sequences is required for understanding the histories of toxin. Determination of their boundaries is still a difficult problem based on limited experimental knowledge in most cases. Thanks to our previous proteomics work [14], in which 24 toxins were fully and 10 toxins partially sequenced, we were able to decide precursor endoproteolytic sites and amidation with high confidence, as shown in Figure 1.

Classification of the CKTs

The CKTs of the *C. jingzhao* ESTs were firstly classified into two groups. One class includes 76 sequences with at least one homolog in our data and high sequence similarity to certain known toxins. The others are grouped into an orphan family including 19 sequences. The sequences of the two groups were clustered to construct a phylogenetic tree separately using ClustalW with manual revision. As shown in Figure 2, toxins in the first group can be classified into six families, A–F, based on the phylogenetic analysis. In the orphan family, five styles of CKTs are categorized according to the cysteine arrangement of the mature peptides (Fig. 1). The characters of the families are summarized in Table 1.

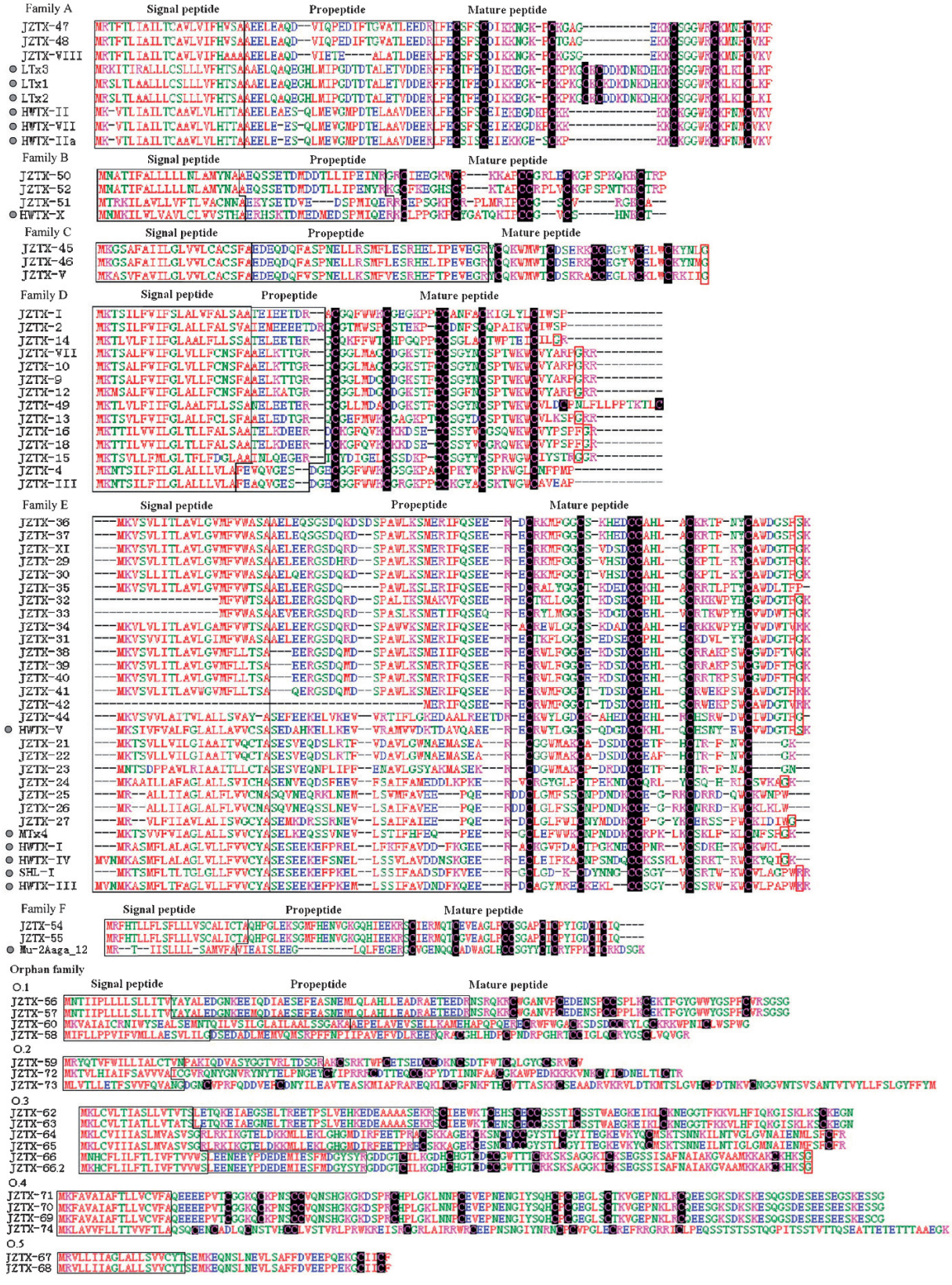

Figure 1. Sequence alignment of representative cystine knot toxin (CKT) precursors. Signal peptide and propeptide are boxed and cysteines of mature peptide are in shadow. The homologies to other spiders are remarked by gray circles. Gaps (dashes) were introduced to maximize the deduced polypeptide sequence similarities. Rectangles denote C-terminal amidation. Hydrophobic residues are shown in red, polar uncharged residues in green, basic residues in pink and acidic residues blue. The orphan sequences are not aligned because of low sequence similarity among them.

Table 1. Sequence diversity of the cystine knot toxins in *Chilobrachys jingzhao*

Family	Signal peptide mode	Length of propeptides	Cysteine arrangement	Polyadenylation signal	Hydrophobic surface
A	MR/K $hTh_{5-6}CS/TS\ h_{5-6}HTS/T$ **A**	26–28	-**C**-**C**-**C**-**C**-**C**-**C**-	AATAAA	N[c]
B	$Mphph_8ph_3p_{2-3}$**A**	17–20	-**C**-**C**-**CC**-**C**-**C**-	ATTAAA	N
C	$MKh_{0-1}p_{1-2}\ h_6Gh_4ChCph$**A**	32	-**C**-**C**-**CC**-**C**-**C**-	ATTAAA-AATAAA	Y
D	$MKp_{1-3}\ h_{5-7}ph_{5-7}\ p_{1-3}\ h_{1-2}$**A**	<10	-**C**-**C**-**CC**-**C**-**C**-(**C**-**C**)	AATAAA	Y
E	$MK/RhS(h_3T)h_{1-6}Gh_{4-7}p_{1-2}$**A**	25–31	-**C**-**C**-**CC**-**C**-**C**-	AATAAA	Y
F	$MRh(H)Th_{2-4}S\ h_{4-5}S(C)h_{3-4}(CT)$**A**	18–25	-**C**-**C**-**CC**-**C**-**C**-**C**-**C**-	AATAAA	N
O.1	–[a]	25–43	-**C**-**C**-**CC**-**C**-**C**-	AATAAA	Y/N
O.2	–[a]	20/UK[b]	-**C**-**C**-**CC**-**C**-**C**-**C**-**C**-	AATAAA	Y/N
O.3	–[a]	24–36	-**C**-**C**-**C**-**CC**-**C**-**C**-**C**-	AATAAA	N
O.4	–[a]	UK	-**C**-**C**-**CC**-**C**-**C**-**C**-**C**-**C**-**C**-	AATAAA	N
O.5	–[a]	UK	-**C**-**C**-	AATAAA	Y

In the signal peptide mode, 'h' indicates hydrophobic residue, 'p' represents polar uncharged residue, and the Arabic numerals denote the number of residues. The other capitals indicate the corresponding amino acids.
[a] There is no common mode because of limited similarity among the members of orphan family.
[b] UK means unknown.
[c] N, no hydrophobic surface; Y, yes.

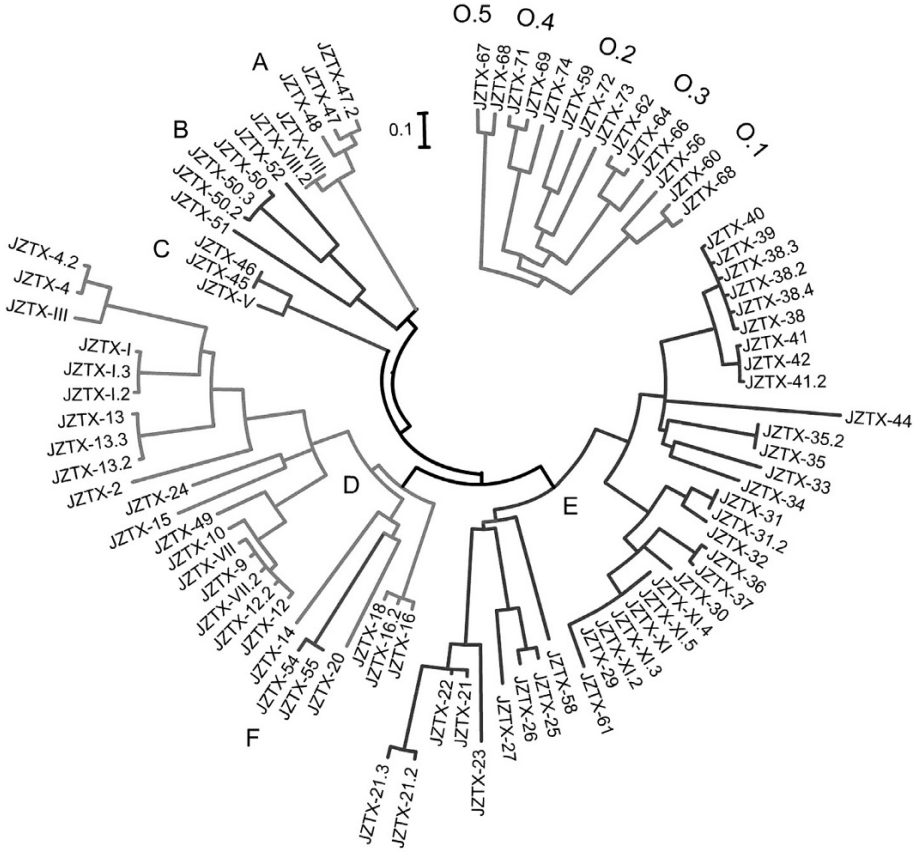

Figure 2. Complete alignment phylogenetic tree with manual revision generated from tarantula *C. jingzhao* CKT precursors.

Family A. The family includes a known toxin JZTX-VIII and two new ones (JZTX-47 and JZTX-48). JZTX-47 and JZTX-48 are native mutants that differ by only one amino acid in the mature peptide. They differ from JZTX-VIII mainly in the propeptide region. The major feature of the family is a putative DDH-derived fold characterized by a special disulfide pairing at C_I–C_{III}, C_{II}–C_V, and C_{IV}–C_{VI} (C represents cysteine residue). The DDH-derived fold toxin was first found in *Ornithoctonus huwena* as HWTX-II [11].

So far, nine toxin precursors with a DDH-derived fold (including the toxins of family A) from three different genera of tarantula have been identified. The similarities of the amino acid sequence and the 3′ untranslated region (UTR) among them are more than 64% and 50%, respectively. The signal sequences of all DDH-derived fold toxins are 22 residues in length,

and the construction mode can be denoted as a model: MR/K $hTh_{5-6}CS/TS\ h_{5-6}HTS/T\ A$ (Where 'h' indicates a hydrophobic residue, and the Arabic numerals denote the number of residues; other capitals indicate the amino acid). The pro-region of this family has 26–28 residues, ending in three acidic residues followed by arginine.

Family B. Family B includes JZTX-51 and two homologous sequences. Their signal peptides are characterized by the second residue being uncharged (Asn/Thr) rather than the conserved basic residues (Arg/Lys) in other categories. Their construction can be denoted as a model: '$Mphph_8ph_3p_{2-3}A$' as described above, where p is a polar uncharged residue. They have propeptides with 17–20 residues. The polyadenylation signal located at 10–30 bases upstream of polyA is thought to control mRNA cleavage by forming a protein complex with the cleavage and polyadenylation specificity factor [33]. In contrast to other families, the family B has a distinct polyadenylation signal 'ATTAAA' in the 3' UTR but not the common one 'AATAAA'. This was also found in the homolog HWTX-X from *O. huwena.*

In the mature peptides, family B follows an ICK motif and has great sequence diversity. No contiguous hydrophobic residues are found between C_I and C_{II} residues, which are thought pivotal to form a hydrophobic surface to interact with voltage sensors of ion channel [34, 35]. This character suggests that they may function as blockers to certain ion channels.

Family C. Family C contains JZTX-V and two new toxins that have significant similarity to some well-known toxins from three genera of tarantula such as ProTx-II (Swiss-Prot accession P83476), GsMTx-2 (P60273), Phrixotoxin-1 (P61230), peptide GsAF 1 (P61408) and peptide GsAF 2 (P61409). Although, sequence alignment indicates that the eight mature peptides can exhibit high sequence homology with each other (Supplemental figure, http://protchem.hunnu.edu.cn/Labweb/Publication/Pub_material.htm), their functions are significantly divergent (or uncertain) [36–38]. The major characteristic of family C is the conserved sequence motif "YCQKW" in the N terminus of the mature peptides. In contrast to the mature peptides of other three families, the toxins in family C have only three residues in the loop between C_V and C_{VI}, which were defined as "short loop tarantula ICKs" [3]. There are three contiguous hydrophobic residues between C_I and C_{II} residues and two contiguous hydrophobic residues following C_{VI} residue. The hydrophobic structures play an important function when the toxins act with the channels [34, 35].

The candidates in this family usually have long pro-regions that are composed of 32 amino acids and end with Glu-Gly-Arg. The polyadenylation signals of family C are tandem with an 'AATAAA' and an 'ATTAAA' in 3′ UTR.

Family D. Family D is a large family of CKTs (24 distinct sequences) including two important components of the venoms (JZTX-I and JZTX-III), which have been chemically and functionally characterized in our previous work [27, 28]. However, the family may be narrowly distributed because so far no homologs from other spiders have been found. The signal peptides of family D show a high sequence identity (over 50 %), and the arrangement mode of the signal peptides can be denoted using a model as described above: $MKp_{1-3}h_{5-7}ph_{5-7}\ p_{1-3}h_{1-2}A$. The pro-regions of the family are short with less than ten amino acid residues.

There are two or three contiguous hydrophobic residues between C_I and C_{II} residues (except in JZTX-15, 16 and 18, where the hydrophobic residues are separated), a hydrophobic residue at the C terminus and two at the N terminus of C_{VI} residue. Interestingly, JZTX-49 possesses two additional cysteines in its long C-terminal region and has great sequence similarity with other family D toxins (e.g., 63 % to JZTX-9).

Family E. Family E is the largest family of CKT in the venom of *C. jingzhao* that contains 37 toxins. The construction mode of the signal peptide can be denoted using a model as described above, MK/$RhS(h_3T)h_{1-6}Gh_{4-7}p_{1-2}A$. Composed of 25–31 residues, the pro-region of the family usually contains a sequence motif "Glu-Glu-Arg" at its end. The mature peptides in family E also have an ICK motif with a putative hydrophobic surface as do families C and D. There are two or three contiguous hydrophobic residues between C_I and C_{II} residues (except in JZTX-44, in which the hydrophobic residues are separated), and one or two hydrophobic residues at the C terminus. Compared with family D, family E is rich in acidic residues in the region between C_{II} and C_{III} residues, a property that has been proved to crucial for interaction with ion channels [8, 35].

Six toxin homologs (HWTX-V, SHL-I, HWTX-I, HWTX-III, HWTX-IV and GsMTx-4, Swiss-Prot accessions are P61104, Q86C51, P56676, P61103, P83303 and Q7YT39 respectively) of this family were found, implying that the toxins belonging to family E may be distributed widely in spider glands.

Family F. The family includes two mu-agatoxin-like peptides (JZTX-54 and JZTX-55), which have eight

cysteines and a typical motif emerging in mu-agatoxin ("$C_V X1 C_{VI} X5 C_{VII} X1 C_{VIII}$" where X is any residue except cystine). Mu-agatoxins were first found in *Agelenopsis aperta* venom [39]. Recently, several homologs of mu-agatoxin were identified in Australian funnel-web spiders (*Atrax robustus*) [40]. The same scaffold is also widely adopted by other spider toxins, such as ω-Aga-IV (*Agelenopsis aperta*) [41], PNTx3–2, PRTx22C5 (*Phoneutria nigriventer*) [42], LiTx2 (*Loxosceles intermedia*) [43], δ-paluIT4 *(Paracoelotes luctuosus*) [44] and the toxin AcTx (*Hadronyche infensa*) [45]. JZTX-54 and JZTX-55 may be the first mu-agatoxin-like peptides reported from the venom of tarantula spider. However, the signal peptides and propeptides of these toxins from different infra-order spiders do not have as high sequence similarity as the former five families. Figure 1 showed that mu-2Aaga-12 had the higher sequence similarity with JZTX-54, 55 in family F. Mature peptide of JZTX-54 had been purified from the crude venom of *C. Jingzhao* spider and the MALDI-TOF MS as well as Edman degradation result confirmed its presence and the full-length of amino acid sequence [14].

Orphan family. Most of the toxins in the orphan family were first identified from the venom of spider and exhibit low sequence similarity with each other. Here, we have classified them into five groups based on the arrangement of cysteines in mature peptide: (1) -C-C-CC-C-C-, JZTX-56, JZTX-57, JZTX-58 and JZTX-60. This kind of the cysteine arrangement is similar to that of most ICK (knottin) toxins frequently emerging in spider and cone snail venoms, and the amino acid sequences of their prepro-regions exhibit limited similarity with those of the four families mentioned above; (2) -C-C-CC-C-C-C-C-, JZTX-59, JZTX-72 and JZTX-73. There are eight cysteine residues in these toxins, and the residues in every loop vary greatly; (3) -C-C-C-CC-C-C-C-, JZTX-62, JZTX-63, JZTX-64, JZTX-65, JZTX-66 and JZTX-66.2. The cysteine arrangement looks like the "long loop ICK" toxins [3] with two epactal cysteines (C_{III} and C_{VIII}); (4) -C-C-CC-C-C-C-C-C-C, JZTX-69, JZTX-70, JZTX-71 and JZTX-74. Their conspicuous characteristic is a cysteine-rich sequence followed by a repetitive sequence with no cysteines; and (5) –C-C-, JZTX-67 and JZTX-68. They may have very short mature peptides and are homologous to the N terminus of JZTX-27. The analogous propeptides as well as their processing sites are still unknown. Among them, JZTX-63 and JZTX-66 had been purified from the venom of *C. jingzhao* and determined by MALDI-TOF MS and N-terminal sequencing [14].

Function diversity on rat DRG neurons

Explorating the functions of these new toxins further, we observed the actions of 10 representative toxins, purified from *C. jingzhao* venom, on Nav, Kv and Cav channels of rat DRG neurons using the whole-cell patch-clamp technique. In addition, the actions of four toxins (JZTX-I, JZTX-III, JZTX-V and JZTX-XI) have been reported [27, 28, 46, 47].

In terms of tetrodotoxin (TTX), voltage-gated sodium channels (VGSCs) can be classified into TTX-sensitive (TTX-S) and TTX-resistant (TTX-R) types. Among these toxins, three toxins (JZTX-V, JZTX-45 and JZTX-32) at 1 μM inhibited both TTX-S Na^+ currents and TTX-R Na^+ currents in rat DRG neurons, while 1 μM JZTX-34 and 1 μM JZTX-54 could only inhibit TTX-S Na^+ currents (Fig. 3A, B). There are two main categories of voltage-gated calcium channels (VGCCs) in rat DRG neurons: low-voltage-activated (LVA) calcium channels (T-type) and high-voltage-activated (HVA) channels (L-, N-, P-, Q- and R-type channels) [48–51]. As seen in Figure 3C, representative toxins exhibited no evident effects on HVA calcium channels in rat DRG neurons, and only JZTX-32 had an effect on HVA calcium currents in rat DRG neurons. The perfusion of 1 μM JZTX-32 inhibited HVA currents by $50.2 \pm 1.9\%$. Moreover, no significant alteration was detected on LVA calcium channels before and after the addition of these toxins (data not shown).

Voltage-gated potassium channels (VGPCs) are a diverse and ubiquitous family of membrane proteins expressed in both excitable and nonexcitable cells. Among the toxins, two toxins (JZTX-V and JZTX-34) at 1 μM had obvious effects on VGPCs in rat DRG neurons in this study (Fig. 3D), while other five toxins (JZTX-1, JZTX-III, JZTX-V, JZTX-XI and JZTX-XII) have been reported as gating modifiers of voltage-dependent K^+ channels in our previous work [46, 47, 52].

In conclusion, representative toxins of different superfamilies in our population of venom CKTs can selectively interact with different membrane proteins; similarly, peptides from the same family, differing in amino acid sequence, also exhibited diversity of function. Moreover, we determined the potential targets of four new toxins on mammal sensory neuron membranes in this study.

Structure model comparisons show diverse characters

To elucidate the structural characters of the families, we downloaded known structures and models for each family. Six representative models of six families are shown in Figure 4A. The family A (JZTX-VIII as the representative one) has the DDH-derived fold scaffold and is rich in basic residues. Most of their side

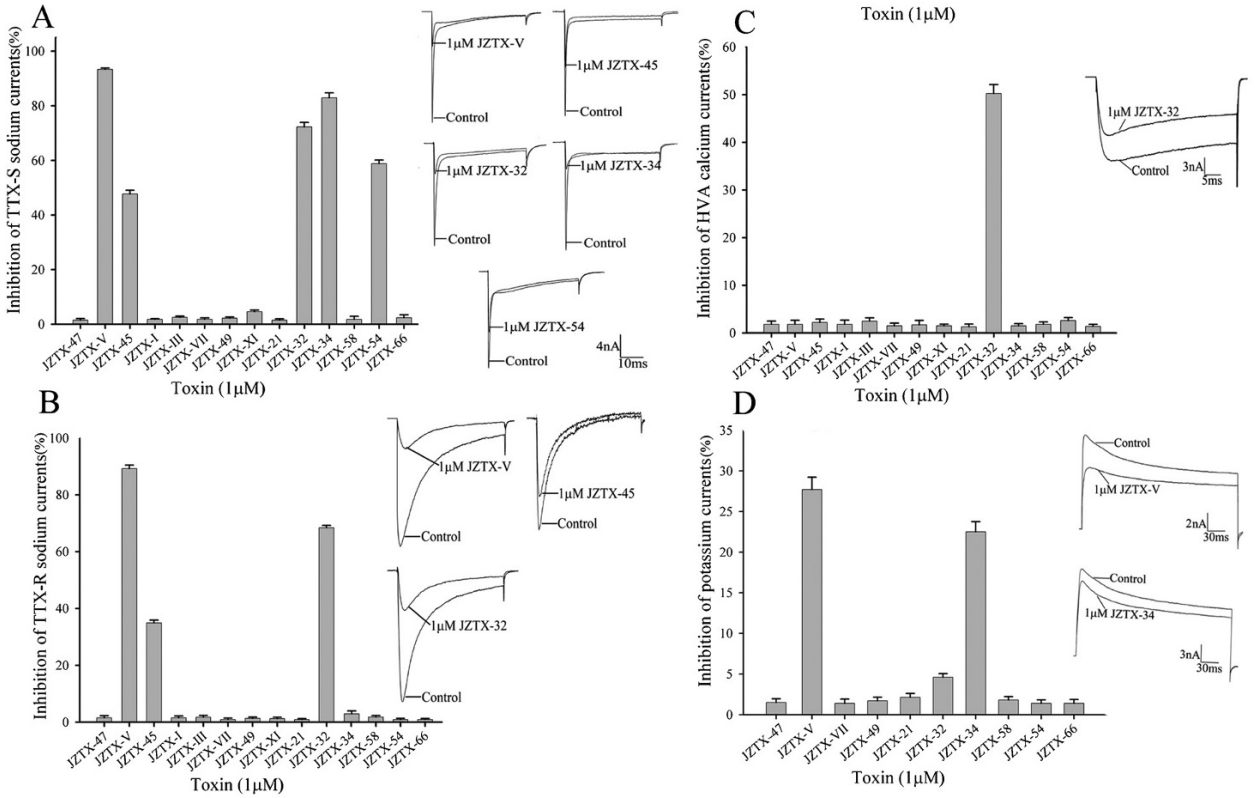

Figure 3. Function diversity of the CKTs of *C. jingzhao*. (*A, B*) Effects of 14 purified toxins on the tetrodotoxin-sensitive (TTX-S) voltage-gated sodium channels (VGSCs) (*A*) and TTX-resistant (TTX-R) VGSCs (*B*) in rat dorsal root ganglion (DRG) neurons. Sodium current traces were evoked by a 50-ms depolarization to –10 mV from a holding potential of –80 mV. JZTX-V, JZTX-45, JZTX-32, JZTX-34 and JZTX-54 at 1 μM inhibited TTX-S Na+ currents by 93.3 ± 0.6 %, 47.7 ± 1.4 %, 72.3 ± 1.6 %, 82.9 ± 1.8 % and 58.8 ± 1.3 %, respectively. In addition, JZTX-V, JZTX-45 and JZTX-32 at 1 μM inhibited TTX-R Na^+ currents by 89.3 ± 1.2 %, 34.9 ± 1.1 % and 68.5 ± 0.8 %, respectively. (*C*) Effects of 14 purified toxins on the voltage-gated calcium channels in rat DRG neurons. Calcium currents were evoked by a 100-ms depolarization to 0 mV from a holding potential of –40 mV. The perfusion of 1 μM JZTX-32 inhibited high-voltage-activated (HVA) calcium currents by 50.2 ± 1.9 %. (*D*) Effects of ten purified toxins on the voltage-gated potassium channels in rat DRG neurons. Potassium currents were elicited at +30 mV from a holding potential of –90 mV. JZTX-V and JZTX-34 at 1 μM inhibited potassium currents by 27.7 ± 1.5 % and 22.5 ± 1.3 %, respectively.

chains are exposed to the outside and may help to form a positive-charged surface of the molecule. This feature is also shared by other DDH-derived fold toxins such as huwentoxin-II, *E. californiacum* toxin 1 and parahybana toxin 1. Other models take the ICK motif as basic scaffold but vary in many aspects. The family F, mu-agatoxin-like toxins (JZTX-54 and 55), has an additional cystine bond and a three-stranded β-sheet. They have a shorter C-terminal region and the typical pattern (CX1CX5CX1C) between C_V and C_{VIII} which is similar to that of other mu-agatoxins. Based on the results of modeling, an additional disulfide bond links the C_{VI} and C_{VII} causing a big loop, which can provide a putative flexible and hydrophobic region for ligand interaction.

The remaining families (B–E) follow the classic ICK motif characterized by the three disulfide bonds pairing of C_I-C_{IV}, C_{II}-C_V, C_{III}-C_{VI} and four loops. Based on previous work [53, 54] and sequence alignment, we defined two sides of the ICK model, one containing a hydrophobic patch (H-side) and the other being the opposite side (O-side). Five polar sites (P1–P5 sites) and four hydrophobic sites (H1–H4 sites) were selected and used to analyze the structural architectures of families of ICK motif toxins (Fig. 4B). The main differences among them consist of the arrangement of hydrophobic and hydrophilic residues. Toxins of family B are rich in basic residues and all the hydrophobic sites are missing with the exception of H2. Therefore, they cannot form a hydrophobic surface. All of the others have the four hydrophobic sites, which form a large conserved hydrophobic surface on one side. Recent research has proved that it is crucial for toxins interacting with plasma membrane [27, 34, 53]. On the O-side, basic residues cluster in families C and D and and acidic residues in family E. The differences result mainly from the replacement of basic residues in families C and D by acidic residues in family E within the P4 site. With additional acidic residues on the P1 and P5 sites, family E may construct

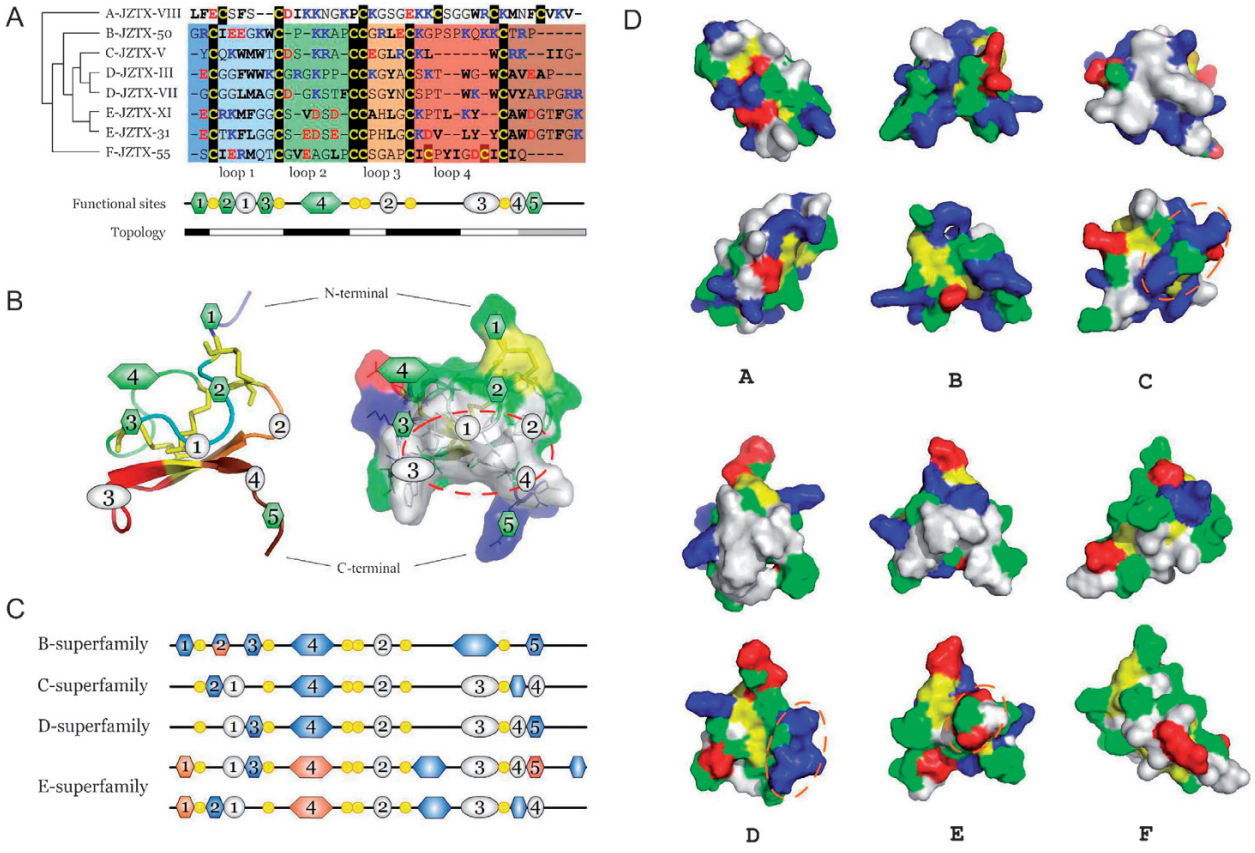

Figure 4. Structural characters of the families. (*A*) Sequence alignment of representative toxins. The sequence portions are colored in rainbow. The Residues forming the hydrophobic surface are bold. The basic and acidic residues are colored by blue and red, respectively. Polar sites (P1 – P5) and hydrophobic sites (H1 – H5) are represented by white ellipses and green hexagons. In the topology bar, black, white and gray regions indicate the sequences in H-side (side with a large hydrophobic surface), the opposite side (O-side) and the not determined, respectively. (*B*) The cartoon and surface model assigned by polar and hydrophobic sites indicating their locations on the 3D structure. The large hydrophobic patch is highlighted by a red ellipse. (*C*) The architectures of four families. Blue and red hexagons represent the basic and acid polar sites, respectively. Some hexagons without number are additional polar sites. (*D*) The surface models of representative toxins from six families (A, JZTX-VII; B, JZTX-50; C, JZTX-V; D, JZTX-III; E, JZTX-XI; F, JZTX-55). In family C, D and E, P4 site on the O-side are highlighted by red cycles.

a negatively charged region. Some research has shown this region may play an important role in inhibiting the deactivation of VGSCs [12, 27]. Family E has two major architectures. One has a positive P3 site and the other has a positive P2 site. They are also different in the C terminus.

Different evolution strategies of family D and family E

In each family, the signal regions exhibit relatively high conservation, whereas the sequences of the mature peptides reveal high diversity. Compared with the signal and the mature peptide, the pro-region has intermediate divergence. This is also observed in conotoxin [55].

To explore evolutionary patterns further, the ratios of Dn/Ds within signal peptide, propeptide and mature peptide were examined separately (Fig. 5). The results indicate most of the ratios of Dn/Ds of family D located in the region lacking constraints, indicating a neutral evolution. As to family E, the ratios within the signal peptide are around 1, indicating neutral evolution. In propeptide regions, most Dn/Ds ratios are smaller than 0.27, implying purifying evolution. Figure 5C and D shows that the ratios of Dn/Ds in small genetic distances (smaller than 0.3) are significant (more than 1) implying positive-selection evolution. The reason for the decrease in the ratio at larger genetic distances is apparently due to saturation. Additionally, we also examined the null hypothesis of the neutral evolution by Fisher's exact test (cut-off 0.05) with Nei and Gojobori model [56] in mature peptide region of the families D and E. No significant results were found in the family D to reject a null hypothesis. In the family E, positive selection was detected in a clade containing eight toxins (JZTX-36, JZTX-37, JZTX-XI, JZTX-29, JZTX-30, JZTX-31, JZTX-20 and JZTX-

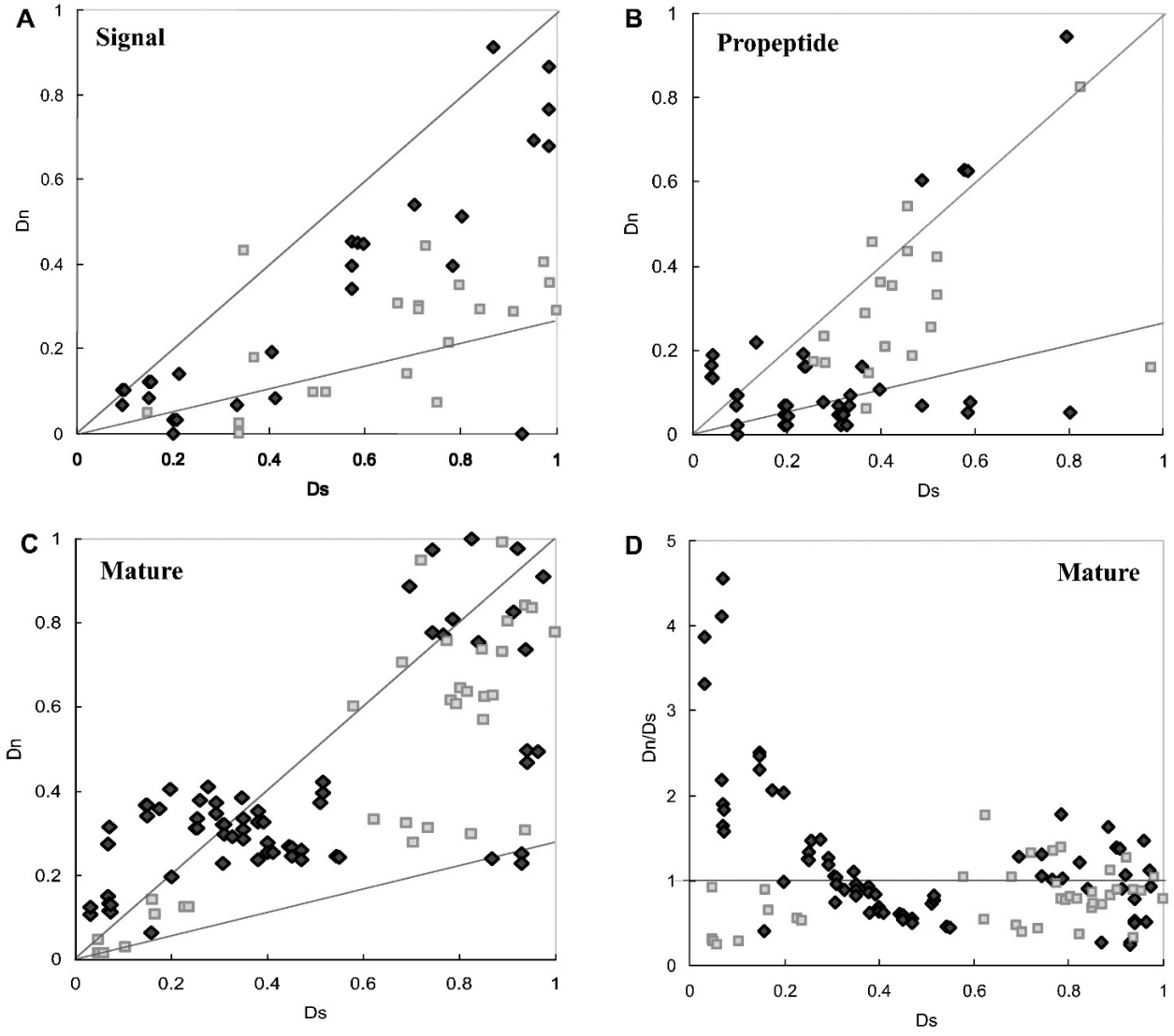

Figure 5. Nonsynonymous versus synonymous substitutions in family D and E. The number of nonsynonymous substitutions per nonsynonymous site (Dn) over number of synonymous substitutions per synonymous site (Ds) about interfamilial comparisons of (*A*) signal, (*B*) propeptide and (*C*) mature peptide encoding domains. The data points of family D and E are color as gray and black, respectively. Lines demarcate zones for Dn/Ds>1 (positive or diversifying selection), 1>Dn/Ds>0.27 (lack of constraints) and Dn/Ds<0.27 (purifying selection). (*D*) Dn/Ds plotted against Ds for the mature domain only note that at Ds>0.3 the signal drops, apparently due to saturation.

61) but was not found in other clades. The present results indicate that the family D has taken neutral evolution and the family E diverse evolution, at least partially.

Unbalanced distribution of toxin abundance among families

The distribution of toxin abundance reflects the composition of venom and is important for understanding of the diversity and evolution of toxins. Recently, our group has reported quantitative data on the toxins of *C. jingzhao*. Quantification of identified peptides was estimated from the percentage (%) of the individual elution peak in the total area under curve, using Millennium32 software (Waters, USA). The data include the ratios of 60 peptide toxins in total, and their sum is 66.8% [52].

As shown in Figure 6A, all the toxins can be categorized into four groups (high, >3%; medium, >1% and <%3; low, >0.5% and <1%; very low <0.5%) according to their abundance. As expected, although some toxins have relative high abundance such as JZTX-I (5.28%), JZTX-III (5.87%), they form a small minority. Many toxins have medium abundance and more have <1%, which indicates that spider venoms are the result of a compromise between efficiency and diversity. To further analysis the abundance of each family, we assigned the 60

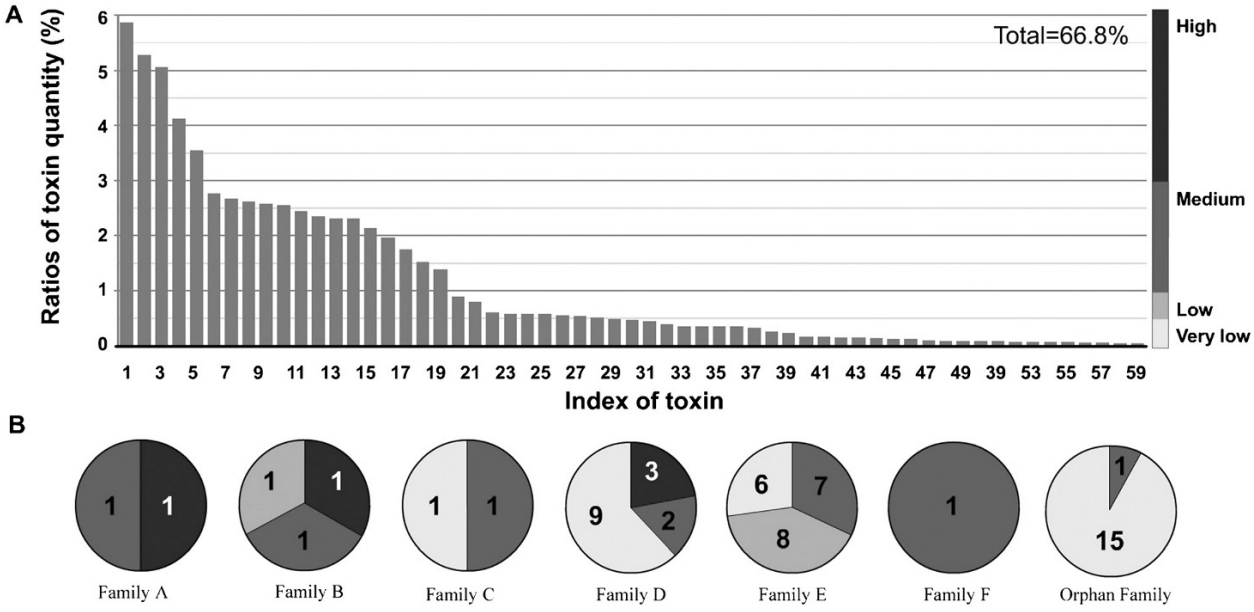

Figure 6. Abundance of venoms components. (*A*) The bar chart of the ratios of 59 toxins quantity. (*B*) Pie charts of the distribution of toxin abundance in six superfamilies. The number of each portion indicates toxin number.

peptide toxins into the families following sequence alignment results. The results reveal that family A, B and F have relatively fewer toxin types but higher mean abundance. Family D contains the 3 highest expressed toxins (JZTX-I, JZTX-III and JZTX-VII) and two other toxins with medium abundance. The remaining 9 have very low abundance. In family E, no highly expressed toxins were found, but 7 and 8 toxins have median and low abundance, respectively. Most of toxins in the orphan family have very low abundance.

Discussion

Biodiversity of spider CKTs

We report 95 novel sequences of CKTs deduced from cDNA sequences. These data increase the number of known nucleotide sequences of tarantula toxin precursor threefold. The phylogenetics and sequence analyses reveal six different superfamilies along with 19 orphan toxins, in which some novel motifs also are found, such as -C-C-CC-C-C-C-C-(C is cysteine), -C-C-C-CC-C-C-C-, as well as longer polypeptides with 10 or 11 cysteines, and with hyper-variable loops between them. These results show the molecular diversity of CKTs in the venom of *C. jingzhao*.

We scanned the activities of 10 toxins on Nav, Kv and Cav channels using whole-cell patch-clamp techniques on rat DRG neurons. Four of these have obvious activities with diverse channel selectivity. This work and some previous experiments [27, 28, 46, 47] reveal the functional diversity of the CKTs from *C. jingzhao*. The toxins without detectable effects on voltage-gated ion channels in DRG cells may affect other types of targets. Examples include some other toxins that have been isolated from *C. jingzhao* venom and characterized, *e.g.*, JZTX-I, a novel neurotoxin preferentially inhibiting cardiac sodium channel inactivation by binding to receptor site 3 [28], rat cardiac TTX-R sodium channel inhibitor JZTX-III [27], and JZTX-XI, a gating modifier of rat cardiac sodium channels [47]. There are also examples of toxins acting on the same channels with different mechanisms. Many toxins of *C. jingzhao* act on a variety of ion channels, also with great selectivity for subtype and binding site. With respect to potential pharmacological applications, these peptides provide promising new templates for further exploration.

Two interaction models of CKTs with channels

According to the structural analysis above and in previous studies, the six families employ different models of interaction between toxin and channel. For example, families B and F are similar to family A in blocking the pore of the channel by electric interaction [29], but in families C, D and E, hydrophobic interaction can aid toxin affinity, for example by first docking to the membrane through their hydrophobic surfaces and then interacting with ion channels using positively or negatively charged residues [27, 34, 53]. The feature of electrostatic anisotropy in the O-side of families C, D and E may be correlated with the different affinity of their ligands, resulting in delay-

ing channel activation or channel deactivation. Therefore, the six families can be categorized into two classes. The first comprises the pore blocking toxins (families A, B and F), which mainly function to prevent interaction with the pore region of various channels. As the pore regions of the same ion channel are usually similar and highly conserved across species, these toxins usually have channel-specific targets in a broad variety of prey and this class has only a few types of toxin. The other class comprises the gating modifiers (families C, D and E), which do not directly block the channels but bind to some regulatory regions of channels such as the "voltage sensor paddle" [34, 57]. This group includes relatively more toxin types and different activities, which follows because the ion channels usually have multiple modifier regions with which the toxin can interact. The combination of the two types of CKTs makes the venoms effective.

The functional studies support our hypothesis that the blocking toxins, comparing with the gate modifiers, usually have more channel-specific functions and narrower targets. As Figure 3 shows, JZTX-54 (family F) has exclusive actions on the TTX-sensitive sodium channel, but gate modifiers such as JZTX-V, JZTX-45 (family C), JZTX-I, JZTX-III (family D) and JZTX-XI, JZTX-32, JZTX-34 (family E) have broad activities. For instance, HWTX-X [29], a homolog of family B, can specifically block the HVA Ca^{2+} currents through GVIA-sensitive, N-type Ca^{2+} channels, whereas it has no detectable effect on other Ca^{2+} channels, or on the voltage-gated Na^{+} and K^{+} channels in rat DRG cells. However, other data suggest that many gate modifiers, such as HaTX [57], GsTxSIA [58], ProTxI, ProTxII [36], *etc.*, which are equipped with a hydrophobic surface, can support a much broader pharmacological profile.

Evolutionary relationships of the CKTs families

The different distribution on species-wide scale of each family based on homologous analysis presents some important clues regarding toxin evolution. The homologies of families A, B, C, E and F have been found in several genera, indicating that these toxins may have existed before the diversion of the families. However, family D may be a young category because so far, it is found only in *C. Jingzhao*.

The abundance analysis reveals that family A, B and F have relatively fewer toxin types but higher mean abundance. This implies that toxins in these families may share a very specific way of interacting with their targets. The wide distribution of families in a number of species (especially family A and F) suggests that their molecular targets/regions may be considerably conserved in various prey (such as insects). In contrast, most of toxins in the orphan family have very low abundance, which hints they may play assistant roles in venoms. Family D has the three most highly expressed toxins, two medium abundance toxins and nine very low abundance toxins. In family E, no highly expressed toxins are found, but seven and eight toxins have median and low abundance respectively. The different levels of abundance in the two families imply that family E may have more functional diversity than family D. If we take their distribution at species-wide scale into account, it is reasonable to predict that family D may have been newly developed to fulfill the special requirement of predation and defense of the *C. JingZhao* spider and family E may be inherited from ancestors to deal with various targets. That family D is subjected to neutral selection looks peculiar, because toxin evolution was commonly thought to be driven by great Darwin positive-selection pressure from the environment. Possible reasons for it may be: (1) since toxin evolution is a combination of positive and negative selections, the Ka/Ks test in a large range may not always obtain significant results especially when these toxins have larger genetic distances; (2) it may be not very surprising that many toxin genes evolved by neutral selection if the environment is relative stable for spiders; (3) the limited sequence data and the mutation saturation may invalidate the method of evolutional analysis. This observation has to be explored further.

Acknowledgments. This project was supported by grants from National Natural Science Foundation of China (NO. 30430170, 30500146 and 30670640) and National 973 Project of China (NO. 2006CB708508). We are grateful for Jixian Xiong, Weijun Hu, Yong Lin and Rui Cao for expert assistance in MALDI-TOF/TOF-MS analysis. We thank Yucheng Xiao, Zhonghua Liu, Ying Wang and Dongyi Zhang for critical reading of the manuscript.

1 Isbister, G. K., Seymour, J. E., Gray, M. R. and Raven, R. J. (2003) Bites by spiders of the family Theraphosidae in humans and canines. Toxicon 41, 519–524.
2 King, G. F. (2004) The wonderful world of spiders: Preface to the special Toxicon issue on spider venoms. Toxicon 43, 471–475.
3 Escoubas, P. and Rash, L. (2004) Tarantulas: Eight-legged pharmacists and combinatorial chemists. Toxicon 43, 555–574.
4 Escoubas, P. (2006) Molecular diversification in spider venoms: A web of combinatorial peptide libraries. Mol. Divers. 10, 545–554.
5 Liang, S. (2004) An overview of peptide toxins from the venom of the Chinese bird spider *Selenocosmia huwena Wang* [=*Ornithoctonus huwena (Wang)*]. Toxicon 43, 575–585.
6 Corzo, G. and Escoubas, P. (2003) Pharmacologically active spider peptide toxins. Cell. Mol. Life Sci. 60, 2409–2426.
7 Rash, L. D. and Hodgson, W. C. (2002) Pharmacology and biochemistry of spider venoms. Toxicon 40, 225–254.
8 Corzo, G., Sabo, J. K., Bosmans, F., Billen, B., Villegas, E., Tytgat, J. and Norton, R. S. (2007) Solution structure and alanine scan of a spider toxin that affects the activation of

mammalian voltage-gated sodium channels. J. Biol. Chem. 282, 4643–4652.
9 Craik, D. J., Daly, N. L. and Waine, C. (2001) The cystine knot motif in toxins and implications for drug design. Toxicon 39, 43–60.
10 Gelly, J. C., Gracy, J., Kaas, Q., Le-Nguyen, D., Heitz, A. and Chiche, L. (2004) The KNOTTIN website and database: A new information system dedicated to the knottin scaffold. Nucleic Acids Res. 32, D156–D159.
11 Shu, Q., Lu, S. Y., Gu, X. C. and Liang, S. P. (2002) The structure of spider toxin huwentoxin-II with unique disulfide linkage: Evidence for structural evolution. Protein Sci. 11, 245–252.
12 Wang, X., Connor, M., Smith, R., Maciejewski, M. W., Howden, M. E., Nicholson, G. M., Christie, M. J. and King, G. F. (2000) Discovery and characterization of a family of insecticidal neurotoxins with a rare vicinal disulfide bridge. Nat. Struct. Biol. 7, 505–513.
13 Kozlov, S. and Grishin, E. (2005) Classification of spider neurotoxins using structural motifs by primary structure features. Single residue distribution analysis and pattern analysis techniques. Toxicon 46, 672–686.
14 Liao, Z., Cao, J., Li, S., Yan, X., Hu, W., He, Q., Chen, J., Tang, J., Xie, J. and Liang, S. (2007) Proteomic and peptidomic analysis of the venom from Chinese tarantula *Chilobrachys jingzhao.* Proteomics 7, 1892–1907.
15 He, Q. Y., He, Q. Z., Deng, X. C., Yao, L., Meng, E., Liu, Z. H. and Liang, S. P. (2008) ATDB: A uni-database platform for animal toxins. Nucleic Acids Res. 36, D293–D297.
16 Diao, J., Lin, Y., Tang, J. and Liang, S. (2003) cDNA sequence analysis of seven peptide toxins from the spider *Selenocosmia huwena.* Toxicon 42, 715–723.
17 Chou, H. H. and Holmes, M. H. (2001) DNA sequence quality trimming and vector removal. Bioinformatics 17, 1093–1104.
18 Sorek, R. and Safer, H. M. (2003) A novel algorithm for computational identification of contaminated EST libraries. Nucleic Acids Res. 31, 1067–1074.
19 Wolfsberg, T. G. and Landsman, D. (1997) A comparison of expressed sequence tags (ESTs) to human genomic sequences. Nucleic Acids Res. 25, 1626–1632.
20 Nishikawa, T., Ota, T., Kawai, Y., Ishii, S., Saito, K., Yamamoto, J., Wakamatsu, A., Ozawa, M., Suzuki, Y., Sugano, S. and Isogai, T. (2002) Database and analysis system for cDNA clones obtained from full-length enriched cDNA libraries. In Silico Biol. 2, 5–18.
21 Gracy, J., Le-Nguyen, D., Gelly, J. C., Kaas, Q., Heitz, A. and Chiche, L. (2008) KNOTTIN: The knottin or inhibitor cystine knot scaffold in 2007. Nucleic Acids Res. 36, D314–D319.
22 Higgins, D. G., Thompson, J. D. and Gibson, T. J. (1996) Using CLUSTAL for multiple sequence alignments. Methods Enzymol. 266, 383–402.
23 Thompson, J. D., Higgins, D. G. and Gibson, T. J. (1994) CLUSTAL W: Improving the sensitivity of progressive multiple sequence alignment through sequence weighting, position-specific gap penalties and weight matrix choice. Nucleic Acids Res. 22, 4673–4680.
24 Sussman, J. L., Lin, D., Jiang, J., Manning, N. O., Prilusky, J., Ritter, O. and Abola, E. E. (1998) Protein Data Bank (PDB): Database of three-dimensional structural information of biological macromolecules. Acta Crystallogr. D Biol. Crystallogr. 54, 1078–1084.
25 Shen, M. Y. and Sali, A. (2006) Statistical potential for assessment and prediction of protein structures. Protein Sci. 15, 2507–2524.
26 DeLano, W. L. (2002) The PyMOL Molecular Graphics System. on World Wide Web http://www.pymol.org.
27 Xiao, Y., Tang, J., Yang, Y., Wang, M., Hu, W., Xie, J., Zeng, X. and Liang, S. (2004) Jingzhaotoxin-III, a novel spider toxin inhibiting activation of voltage-gated sodium channel in rat cardiac myocytes. J. Biol. Chem. 279, 26220–26226.
28 Xiao, Y., Tang, J., Hu, W., Xie, J., Maertens, C., Tytgat, J. and Liang, S. (2005) Jingzhaotoxin-I, a novel spider neurotoxin preferentially inhibiting cardiac sodium channel inactivation. J. Biol. Chem. 280, 12069–12076.
29 Liu, Z., Dai, J., Dai, L., Deng, M., Hu, Z., Hu, W. and Liang, S. (2006) Function and solution structure of Huwentoxin-X, a specific blocker of N-type calcium channels, from the Chinese bird spider *Ornithoctonus huwena.* J. Biol. Chem. 281, 8628–8635.
30 Zhang, J., Rosenberg, H. F. and Nei, M. (1998) Positive Darwinian selection after gene duplication in primate ribonuclease genes. Proc. Natl. Acad. Sci. USA 95, 3708–3713.
31 Kumar, S., Tamura, K. and Nei, M. (2004) MEGA3: Integrated software for Molecular Evolutionary Genetics Analysis and sequence alignment. Brief Bioinform. 5, 150–163.
32 Leisy, D. J., Mattson, J. D., Quistad, G. B., Kramer, S. J., Van Beek, N., Tsai, L. W., Enderlin, F. E., Woodworth, A. R. and Digan, M. E. (1996) Molecular cloning and sequencing of cDNAs encoding insecticidal peptides from the primitive hunting spider, *Plectreurys tristis* (Simon). Insect Biochem. Mol. Biol. 26, 411–417.
33 Proudfoot, N. J. and Brownlee, G. G. (1976) 3' non-coding region sequences in eukaryotic messenger RNA. Nature 263, 211–214.
34 Lee, S. Y. and MacKinnon, R. (2004) A membrane-access mechanism of ion channel inhibition by voltage sensor toxins from spider venom. Nature 430, 232–235.
35 Wang, J. M., Roh, S. H., Kim, S., Lee, C. W., Kim, J. I. and Swartz, K. J. (2004) Molecular surface of tarantula toxins interacting with voltage sensors in K(v) channels. J. Gen. Physiol. 123, 455–467.
36 Middleton, R. E., Warren, V. A., Kraus, R. L., Hwang, J. C., Liu, C. J., Dai, G., Brochu, R. M., Kohler, M. G., Gao, Y. D., Garsky, V. M., Bogusky, M. J., Mehl, J. T., Cohen, C. J. and Smith, M. M. (2002) Two tarantula peptides inhibit activation of multiple sodium channels. Biochemistry 41, 14734–14747.
37 Oswald, R. E., Suchyna, T. M., McFeeters, R., Gottlieb, P. and Sachs, F. (2002) Solution structure of peptide toxins that block mechanosensitive ion channels. J. Biol. Chem. 277, 34443–34450.
38 Chagot, B., Escoubas, P., Villegas, E., Bernard, C., Ferrat, G., Corzo, G., Lazdunski, M. and Darbon, H. (2004) Solution structure of Phrixotoxin 1, a specific peptide inhibitor of Kv4 potassium channels from the venom of the theraphosid spider *Phrixotrichus auratus.* Protein Sci. 13, 1197–1208.
39 Skinner, W. S., Adams, M. E., Quistad, G. B., Kataoka, H., Cesarin, B. J., Enderlin, F. E. and Schooley, D. A. (1989) Purification and characterization of two classes of neurotoxins from the funnel web spider, *Agelenopsis aperta.* J. Biol. Chem. 264, 2150–2155.
40 Escoubas, P., Sollod, B. and King, G. F. (2006) Venom landscapes: Mining the complexity of spider venoms via a combined cDNA and mass spectrometric approach. Toxicon 47, 650–663.
41 Adams, M. E., Mintz, I. M., Reily, M. D., Thanabal, V. and Bean, B. P. (1993) Structure and properties of omega-agatoxin IVB, a new antagonist of P-type calcium channels. Mol. Pharmacol. 44, 681–688.
42 Kalapothakis, E., Penaforte, C. L., Leao, R. M., Cruz, J. S., Prado, V. F., Cordeiro, M. N., Diniz, C. R., Romano-Silva, M. A., Prado, M. A., Gomez, M. V. and Beirao, P. S. (1998) Cloning, cDNA sequence analysis and patch clamp studies of a toxin from the venom of the armed spider (*Phoneutria nigriventer*). Toxicon 36, 1971–1980.
43 de Castro, C. S., Silvestre, F. G., Araujo, S. C., Gabriel de, M. Y., Mangili, O. C., Cruz, I., Chavez-Olortegui, C. and Kalapothakis, E. (2004) Identification and molecular cloning of insecticidal toxins from the venom of the brown spider *Loxosceles intermedia.* Toxicon 44, 273–280.
44 Corzo, G., Escoubas, P., Stankiewicz, M., Pelhate, M., Kristensen, C. P. and Nakajima, T. (2000) Isolation, synthesis and pharmacological characterization of delta-palutoxins IT, novel insecticidal toxins from the spider *Paracoelotes luctuosus* (*Amaurobiidae*). Eur. J. Biochem. 267, 5783–5795.

45 Rosengren, K. J., Wilson, D., Daly, N. L., Alewood, P. F. and Craik, D. J. (2002) Solution structures of the cis- and trans-Pro30 isomers of a novel 38-residue toxin from the venom of Hadronyche Infensa sp. that contains a cystine-knot motif within its four disulfide bonds. Biochemistry 41, 3294–3301.
46 Yuan, C., Liao, Z., Zeng, X., Dai, L., Kuang, F. and Liang, S. (2007) Jingzhaotoxin-XII, a gating modifier specific for Kv4.1 channels. Toxicon 50, 646–652.
47 Liao, Z., Yuan, C., Deng, M., Li, J., Chen, J., Yang, Y., Hu, W. and Liang, S. (2006) Solution Structure and Functional Characterization of Jingzhaotoxin-XI: A novel gating modifier of both potassium and sodium channels. Biochemistry 45, 15591–15600.
48 Llinas, R., Sugimori, M., Lin, J. W. and Cherksey, B. (1989) Blocking and isolation of a calcium channel from neurons in mammals and cephalopods utilizing a toxin fraction (FTX) from funnel-web spider poison. Proc. Natl. Acad. Sci. USA 86, 1689–1693.
49 Nowycky, M. C., Fox, A. P. and Tsien, R. W. (1985) Three types of neuronal calcium channel with different calcium agonist sensitivity. Nature 316, 440–443.
50 Wheeler, D. B., Randall, A. and Tsien, R. W. (1994) Roles of N-type and Q-type Ca^{2+} channels in supporting hippocampal synaptic transmission. Science 264, 107–111.
51 Zhang, J. F., Randall, A. D., Ellinor, P. T., Horne, W. A., Sather, W. A., Tanabe, T., Schwarz, T. L. and Tsien, R. W. (1993) Distinctive pharmacology and kinetics of cloned neuronal Ca^{2+} channels and their possible counterparts in mammalian CNS neurons. Neuropharmacology 32, 1075–1088.
52 Yuan, C., Yang, S., Liao, Z. and Liang, S. (2007) Effects and mechanism of Chinese tarantula toxins on the Kv2.1 potassium channels. Biochem. Biophys. Res. Commun. 352, 799–804.
53 Takahashi, H., Kim, J. I., Min, H. J., Sato, K., Swartz, K. J. and Shimada, I. (2000) Solution structure of hanatoxin1, a gating modifier of voltage-dependent K(+) channels: Common surface features of gating modifier toxins. J. Mol. Biol. 297, 771–780.
54 Maggio, F. and King, G. F. (2002) Scanning mutagenesis of a Janus-faced atracotoxin reveals a bipartite surface patch that is essential for neurotoxic function. J. Biol. Chem. 277, 22806–22813.
55 Zhang, B., Liu, Q., Yin, W., Zhang, X., Huang, Y., Luo, Y., Qiu, P., Su, X., Yu, J., Hu, S. and Yan, G. (2006) Transcriptome analysis of *Deinagkistrodon acutus* venomous gland focusing on cellular structure and functional aspects using expressed sequence tags. BMC Genomics 7, 152.
56 Nei, M. and Gojobori, T. (1986) Simple methods for estimating the numbers of synonymous and nonsynonymous nucleotide substitutions. Mol. Biol. Evol. 3, 418–426.
57 Li-Smerin, Y. and Swartz, K. J. (2000) Localization and molecular determinants of the Hanatoxin receptors on the voltage-sensing domains of a K(+) channel. J. Gen. Physiol. 115, 673–684.
58 Li-Smerin, Y. and Swartz, K. J. (1998) Gating modifier toxins reveal a conserved structural motif in voltage-gated Ca^{2+} and K^{+} channels. Proc. Natl. Acad. Sci. USA 95, 8585–8589.